Hindawi
International Journal of Aerospace Engineering
Volume 2022, Article ID 1000865, 15 pages
https://doi.org/10.1155/2022/1000865

Research Article

A Fast Algorithm for Determining the Optimal Navigation Star for Responsive Launch Vehicles

Yi Zhao,[1] **Hongbo Zhang**,[1] **Pengfei Li**,[2] **and Guojian Tang**[1]

[1]*College of Aerospace Science and Engineering, National University of Defense Technology, 410073, China*
[2]*Strategic Support Force Space Systems Department Staff, 100000, China*

Correspondence should be addressed to Hongbo Zhang; zhanghb1304@nudt.edu.cn

Received 28 October 2021; Accepted 14 March 2022; Published 19 April 2022

Academic Editor: Fangzhou Fu

The platform inertial-stellar composite guidance is a composite guidance method supplemented by stellar correction on the basis of inertial navigation, which can effectively improve the accuracy of responsive launch vehicles. In order to solve the problem of rapid determining the optimal navigation star in the system, this paper proposes an algorithm based on the equivalent information compression theory. At first, this paper explains why the single-star scheme can achieve the same accuracy as the dual-star scheme. At the same time, the analytical expression of the optimal navigation star with significant initial error is derived. In addition, the available optimal navigation star determination strategy is also designed according to the arrow-borne navigation star database. The proposed algorithm is evaluated by two representative responsive launch vehicle trajectory simulations. The simulation results demonstrate that the proposed algorithm can determine the optimal navigation star quickly, which greatly shorten the preparation time before the rapid launch of vehicles and improve the composite guidance accuracy.

1. Introduction

Inertial-stellar composite guidance is a composite guidance method based on inertial guidance supplemented by stellar guidance. It utilizes the inertial space azimuth datum provided by the star to calibrate the error angle between the platform coordinate system and the launch inertial coordinate system and corrects the impact point deviation caused by the platform pointing error [1]. Inertial-stellar composite guidance system corrects the drift error of inertial platform according to the star sensor information, which can not only improve the guidance accuracy and rapid launch ability [2] but also reduce the cost. Moreover, the motion parameters of spacecraft in space can be determined [3–5], and it has strong environmental adaptability.

Inertial-stellar guidance is essentially a problem of determining attitude through vector observation. This problem was first proposed by Wahba [6], and various attitude determination algorithms were developed, such as TRIAD [7], QUEST [8, 9], SVD [10], FOAM [11], Euler-q [12], and fast linear attitude estimator method [13–15]. In order to solve the case that there are a large number of outliers, Yang and Carlone formulated the Wahba problem by truncated least squares [16]. Ghadiri et al. [17] proposed a robust multi-objective optimization method to overcome the static attitude determination with bounded uncertainty. These algorithms need at least two vector information to calculate the attitude. However, in some cases, long-term observation of one vector is enough [18]. Reference [19] proposed an attitude determination algorithm based on the minimum squares sum of image point coordinate residuals. The algorithm can still determine the attitude when only one star is observed. Reference [20] derived the attitude analytical solution when only one sensor is used for observation. The analytical solution can be expressed by the combination of two limiting quaternions, and the covariance and singularity analyses were carried out. However, it did not determine the optimal attitude solution. Similarly, according to the number of observation vectors, the inertial-stellar composite guidance can also be divided into single vector observation and double vectors observation, that is, single-star scheme and double-star scheme. For the platform inertial navigation system, the star sensor is usually fixedly installed on the platform. Because the direction of the platform in the inertial space cannot be adjusted after launch, the double-star scheme needs to install two star sensors on the platform, which will greatly complicate the structure. It is found that observing the specific direction star, the single-star scheme can achieve the same accuracy as the double-star scheme [21, 22]. Zhang et al. have proved it theoretically [23]. As it is known, the only practical application is the single-star scheme, such as the American "Trident" submarine long-range ballistic missile. However, the single-star scheme needs to determine the optimal navigation star before the vehicle launch. At present, the optimal navigation star is determined by numerical method [24, 25], which increases the preparation time and limits the wide application.

Motivated by the work of Zhang et al., this paper proposes a fast algorithm to determine the optimal navigation star for responsive launch vehicles. Firstly, the relationship equations between the initial error and the impact point deviation and the star sensor measurement are established. Then, our algorithm exploits the equivalent information compression theory [23] to explain why the single-star scheme can achieve the accuracy as the double-star scheme and deduces the optimal navigation star under the condition of significant initial error. The deduced analytical solution can greatly shorten the pre-launch preparation time. On this basis, the local navigation star database is determined according to the deviation angle, and the available optimal navigation star can be determined.

The structure of this paper is as follows. Section 2 presents the definitions of various coordinate system and the derivations of inertial platform system and star sensor model. Section 3 shows the analytical expression of the optimal navigation star. In Section 4, the available optimal navigation star is determined based on the arrow-borne navigation star database. The simulation results and conclusions are given in Section 5 and Section 6. The contribution of this paper is to provide an analytical solution of optimal navigation star to shorten the prelaunch preparation time and enhance the performance for responsive launch vehicles.

2. Inertial Platform System and Star Sensor Modeling

2.1. Definitions of Various Coordinate System

2.1.1. Geocentric Inertial Coordinate System $o_E - x_I y_I z_I$. The coordinate system origin o_E is the earth centroid, and the basic plane is the J2000 earth equatorial plane. The $o_E x_I$ axis points from the earth centroid to the J2000 mean equinox in the basic plane. The $o_E z_I$ axis points to the north pole along the normal of the basic plane. The $o_E y_I$ axis and the other two axes constitute the right hand system. This coordinate system is abbreviated as the i-system.

2.1.2. Launch Coordinate System $o - xyz$. The system mainly describes the motion of responsive launch vehicle relative to the earth. The launch coordinate system is fixedly connected with the earth, and the origin is taken as the launch point o. In the system, the ox axis points to the launch aiming direction in the launch horizontal plane, the oy axis points upward perpendicular to the launch point horizontal plane, and the oz axis is perpendicular to the xoy plane. The axes ox, oy, and oz form the right hand coordinate system. This coordinate system is abbreviated as the g-system (Figure 1).

2.1.3. Launch Inertial Coordinate System $o_A - x_A y_A z_A$. The launch inertial coordinate system coincides with the launch coordinate system at the launch time. But after launching the vehicle, the origin and the direction of each axis remain stationary in the inertial space. The coordinate system is used to establish the vehicle motion equation in inertial space. This coordinate system is abbreviated as the A-system.

2.1.4. Ideal Inertial Platform Coordinate System $o_{P'} - x_{P'} y_{P'} z_{P'}$. The coordinate system origin $o_{p'}$ is located at the platform datum, and the coordinate axis is defined by the platform frame axis or the gyro-sensitive axis. After pre-launch alignment and leveling, each coordinate axis shall be parallel to each coordinate axis of the launch inertial coordinate system. This coordinate system is abbreviated as the p'-system.

2.1.5. Inertial Platform Coordinate System $o_P - x_P y_P z_P$. Due to the platform misalignment angle, there is a deviation between the inertial platform coordinate system and the ideal inertial platform coordinate system. This coordinate system is abbreviated as the p-system.

2.1.6. Star Sensor Coordinate System $o_s - x_s y_s z_s$. The coordinate system mainly describes the star sensor measurement. In the system, the coordinate system origin o_s is at the centre of the star sensor imaging device (charge couple device, complementary metal oxide semiconductor, etc.). The $o_s x_s$ axis is consistent with the axis of the optical lens, the $o_s y_s$ axis is the vertical to the pixel readout direction, and the $o_s z_s$ axis is the horizontal to the pixel readout direction. The $y_s o_s z_s$ plane is consistent with the imaging device plane. The transformation matrix between the star sensor coordinate system and the vehicle body coordinate system is determined by the star sensor installation angle. This coordinate system is abbreviated as the s-system.

2.2. Relationship between Impact Point Deviation and Platform Misalignment Angle. The platform misalignment angle represents the inertial reference deviation, that is, the error angle between the inertial platform and the launch inertial coordinate system. It is mainly caused by various initial errors and inertial navigation errors and affects the landing point accuracy. Although the platform misalignment angle is affected by many factors, the initial error accounts for the main part under certain conditions. For the rapid maneuvering launch vehicle, the accuracy of pre-launch orientation and alignment may not be very high, which leads to the significant portion of the initial error in the platform

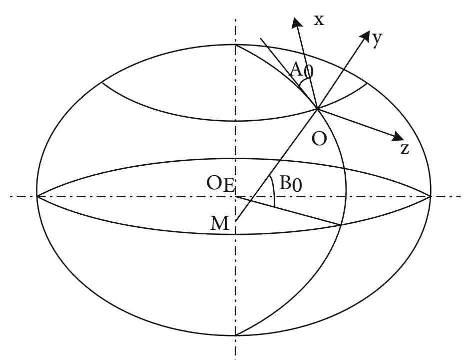

Figure 1: Launch coordinate system.

misalignment angle. Therefore, this paper mainly studies the determination of the optimal navigation star under the significant initial error condition.

The platform inertial system and the launch inertial system can be coincident with the help of the platform initial alignment. The initial alignment error will be caused due to the equipment inherent error, the external interference influence in the alignment process, and the method error. And the platform alignment error around the y-axis will be caused owing to the initial orientation error during launch. Thus, the orientation error can be considered together with the initial alignment error.

The initial alignment and orientation errors can be expressed by the three axis misalignment angles between the p'-system and the A-system, which are defined as$\begin{bmatrix} \varepsilon_{0x} & \varepsilon_{0y} & \varepsilon_{0z} \end{bmatrix}^{\mathrm{T}}$. And there are two parts in ε_{0y}: orientation error and aiming error. It is assumed that the adjustment platform adopts the method of yaw first and then pitch; there is

$$\begin{bmatrix} \alpha_x \\ \alpha_y \\ \alpha_z \end{bmatrix} = \begin{bmatrix} \cos\varphi_r \cos\psi_r & \sin\varphi_r & -\cos\varphi_r \sin\psi_r \\ -\sin\varphi_r \cos\psi_r & \cos\varphi_r & \sin\varphi_r \sin\psi_r \\ \sin\psi_r & 0 & \cos\psi_r \end{bmatrix} \begin{bmatrix} \varepsilon_{0x} \\ \varepsilon_{0y} \\ \varepsilon_{0z} \end{bmatrix} = C_A^{P'} \begin{bmatrix} \varepsilon_{0x} \\ \varepsilon_{0y} \\ \varepsilon_{0z} \end{bmatrix}, \tag{1}$$

where $\begin{bmatrix} \alpha_x & \alpha_y & \alpha_z \end{bmatrix}^{\mathrm{T}}$ are misalignment angles caused by initial alignment and orientation errors, ψ_r and φ_r are the rotation angles around the y-axis and z-axis, respectively, and $C_A^{P'}$ is the transformation matrix from the A-system to the p'-system.

The inertial guidance accuracy meets the following relationship with the initial alignment error:

$$\begin{bmatrix} \Delta L \\ \Delta H \end{bmatrix} = \begin{bmatrix} n_{L1} & n_{L2} & n_{L3} \\ n_{H1} & n_{H2} & n_{H3} \end{bmatrix} \begin{bmatrix} \varepsilon_{0x} \\ \varepsilon_{0y} \\ \varepsilon_{0z} \end{bmatrix}. \tag{2}$$

In which, n_{L1}, n_{L2}, and n_{L3} are the partial derivatives of the longitudinal impact point deviation to the initial errors in three directions, respectively. n_{H1}, n_{H2}, and n_{H3} are the partial derivatives of the lateral impact point deviation to the initial errors in three directions, respectively.

It can be obtained by combining Equation (1) and Equation (2).

$$\begin{bmatrix} \Delta L \\ \Delta H \end{bmatrix} = \begin{bmatrix} q_{11} & q_{12} & q_{13} \\ q_{21} & q_{22} & q_{23} \end{bmatrix} \begin{bmatrix} \alpha_x \\ \alpha_y \\ \alpha_z \end{bmatrix} = \begin{bmatrix} q_1^{\mathrm{T}} \\ q_2^{\mathrm{T}} \end{bmatrix} \begin{bmatrix} \alpha_x \\ \alpha_y \\ \alpha_z \end{bmatrix}. \tag{3}$$

In which,

$$\begin{cases} q_{11} = n_{L1} \cos\varphi_r \cos\psi_r + n_{L2} \sin\varphi_r - n_{L3} \cos\varphi_r \sin\psi_r, \\ q_{12} = -n_{L1} \sin\varphi_r \cos\psi_r + n_{L2} \cos\varphi_r + n_{L3} \sin\varphi_r \sin\psi_r, \\ q_{13} = n_{L1} \sin\psi_r + n_{L3} \cos\psi_r, \\ q_{21} = n_{H1} \cos\varphi_r \cos\psi_r + n_{H2} \sin\varphi_r - n_{H3} \cos\varphi_r \sin\psi_r, \\ q_{22} = -n_{H1} \sin\varphi_r \cos\psi_r + n_{H2} \cos\varphi_r + n_{H3} \sin\varphi_r \sin\psi_r, \\ q_{23} = n_{H1} \sin\psi_r + n_{H3} \cos\psi_r. \end{cases} \tag{4}$$

2.3. Acquisition of Star Sensor Measurement. The elevation and azimuth angle of the optimal navigation star in the A-system are defined as e_s and σ_s, respectively. Thus, the stellar direction unit vector in the A-system can be expressed as

$$S_A = \begin{bmatrix} \cos e_s \cos\sigma_s & \sin e_s & \cos e_s \sin\sigma_s \end{bmatrix}^{\mathrm{T}}. \tag{5}$$

In the s-system, the $o_s x_s$ axis is the optical axis. The angle between the optical axis and the stellar vector is very small, and its directional cosine is approximately 1. The $o_s y_s$ and $o_s z_s$ are the output axes. The stellar vector representation in the star sensor coordinate system is shown in Figure 2. It is assumed that the star sensor outputs are ξ and η; the stellar vector can be expressed as

$$S_S = \begin{bmatrix} 1 & -\xi & -\eta \end{bmatrix}^{\mathrm{T}}. \tag{6}$$

The ideal star sensor output should be $S_{s'} = \begin{bmatrix} 1 & 0 & 0 \end{bmatrix}^{\mathrm{T}}$; then, there is the following equation according to the coordinate transformation relationship:

$$S_{S'} = C_P^S C_A^{P'} S_A, \tag{7}$$

where C_P^S is the transformation matrix from the p-system to the s-system and $C_A^{P'}$ is the transformation matrix from the A-system to the p'-system. According to the stellar vector representation in the A-system and the s-system, the following equation can be obtained by the transformation matrix between different coordinate systems.

$$S_S = C_P^S C_{P'}^P C_A^{P'} S_A, \tag{8}$$

where $C_{P'}^P$ is the transformation matrix from the p'

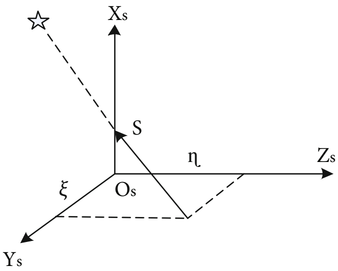

Figure 2: Representation of the stellar vector in the star sensor coordinate system.

-system to the p-system, which can be expressed as

$$C_{P'}^{P} = \begin{bmatrix} 1 & -\alpha_z & \alpha_y \\ \alpha_z & 1 & -\alpha_x \\ -\alpha_y & \alpha_x & 1 \end{bmatrix}. \quad (9)$$

The stellar vector representation in the p-system is defined as S_P, and there is

$$S_P = C_S^P S_S. \quad (10)$$

According to Equation (7), the stellar vector representation in the p'-system can be obtained as follows:

$$S_{P'} = C_S^P S_{S'} = C_A^{P'} S_A. \quad (11)$$

Then, the following equation can be obtained from Equations (10) and (11).

$$\Delta S_P = S_P - S_{P'} = C_S^P (S_S - S_{S'}). \quad (12)$$

And ΔS_p can also be represented as

$$\Delta S_P = S_{P'} \cdot a = \left(C_S^P S_{S'}\right) \cdot a. \quad (13)$$

It can be obtained from Equations (12) and (13).

$$S_s - S_{s'} = C_P^S \left[\left(C_S^P S_{S'}\right) \cdot a\right]. \quad (14)$$

Therefore, the star sensor measurement equation can be expressed as

$$\begin{bmatrix} \xi \\ \eta \end{bmatrix} = \begin{bmatrix} -\sin\psi_0 & 0 & \cos\psi_0 \\ \sin\varphi_0 \cos\psi_0 & -\cos\varphi_0 & \sin\varphi_0 \sin\psi_0 \end{bmatrix} \begin{bmatrix} \alpha_x \\ \alpha_y \\ \alpha_z \end{bmatrix} = \begin{bmatrix} h_1^T \\ h_2^T \end{bmatrix} \begin{bmatrix} \alpha_x \\ \alpha_y \\ \alpha_z \end{bmatrix}, \quad (15)$$

where φ_0 and ψ_0 are the star sensor installation angles.

3. Theoretical Optimal Navigation Star Determination Method

For the platform inertial-stellar composite guidance scheme, the single-star scheme for measuring a special navigation star can achieve the same accuracy as the double-star scheme for measuring two stars. This special star is called the optimal navigation star. In terms of the difficulty and cost of realization, the single-star scheme is definitely better than the double-star scheme. Therefore, the single-star scheme is adopted in the practical engineering, which requires the determination of the optimal navigation star.

In this section, the equivalent information compression theory is utilized to explain why the single-star scheme can achieve the same accuracy as the double-star scheme firstly. Then, the optimal navigation star is further determined based on the principle. Since it is not combined with the navigation star in the star library, it is also called the theoretical optimal navigation star.

3.1. Equivalent Information Compression Theory. The impact point deviation and platform misalignment angle can be expressed in the matrix form

$$p = q \cdot a, \quad (16)$$

where $p = [\Delta L \quad \Delta H]^T$; $q = [q_1 \quad q_2]^T$; and $a = [\alpha_x \quad \alpha_y \quad \alpha_z]^T$. It can be seen from Equation (16) that the rank of q is 2, so there is information compression in the mapping from a to p. It is worth noting that a cannot be uniquely determined by p, which indicates that Equation (16) has numerous solutions. Although there are countless sets of solutions in Equation (16), there is a special solution a_0, which belongs to the subspace $q_s = \text{span}\{q_1 \quad q_2\}$ formed by each row of vectors. Therefore, a_0 can be expressed as

$$a_0 = \alpha_1^0 q_1 + \alpha_2^0 q_2 = q^T \cdot X. \quad (17)$$

Substitute Equation (17) into Equation (16), and there is

$$p = \left(qq^T\right) X. \quad (18)$$

From Equation (17) and Equation (18), we can get

$$a_0 = q^T \left(qq^T\right)^{-1} p. \quad (19)$$

It can be seen from the above equation that a_0 and p correspond to each other one by one. If the inner product of two column vectors is defined as $\langle a \cdot b \rangle = a^T \cdot b$, then Equation (16) can be expressed as

$$p = [\langle q_1 \cdot a \rangle \quad \langle q_2 \cdot a \rangle]^T, \quad (20)$$

where $\langle q_i \cdot a \rangle$ reflects the projection of a in the q_i direction. q_1 and q_2 are linearly independent; therefore, $p = q \cdot a$ reflects the projection a_s of a on space q_s, and the projection information $a_s^\perp$ of a on the orthogonal complement $q_s^\perp$ of q_s is lost. Since q_s is a complete subspace on Hilbert space R^n, there is

$$R^n = q_s + q_s^\perp. \tag{21}$$

According to the projection theorem, we can get

$$a = a_s + a_s^\perp. \tag{22}$$

It can be seen from the relationship between the impact point deviation and the platform misalignment angle that q is not full rank. So only the information a_s in the subspace can be obtained through the impact point deviation, and the information $a_s^\perp$ in the orthogonal complement cannot be obtained.

The star sensor measurement equation can also be expressed in the matrix form

$$Z = h \cdot a. \tag{23}$$

Assuming that another set of bases of q_s is $\{ h_1 \quad h_2 \}$, it can be seen from the above analysis that Z also reflects all the information projected by a on q_s, which can be expressed as

$$a_0 = h^\mathrm{T} \left(hh^\mathrm{T} \right)^{-1} Z. \tag{24}$$

Substitute Equation (24) into Equation (16), and we can get

$$p = q \cdot h^\mathrm{T} \left(hh^T \right)^{-1} Z. \tag{25}$$

Therefore, from the perspective of information compression, q and h are equal compression maps; that is, the impact point deviation p can be uniquely determined by the single-star observation Z.

The impact point deviation is only affected by the projection a_s of the misalignment angle a on the subspace $Q_s = \mathrm{span}\{ q_1 \quad q_2 \}$. Therefore, according to Equation (25), it is only necessary to select h_1 and h_2, so that h and q are equal information compression. Then, the observation information Z contains all the useful information. The schematic diagram of determining the optimal navigation star is shown in Figure 3.

In the figure, all the information of misalignment angle a is composed of a_s and $a_s^\perp$, but only a_s affects the impact point deviation. If h and q are equal information compression maps, the single-star scheme can measure all the information of a_s. Although the double-star scheme can measure all the information of a, only the a_s part is used in the correction, and $a_s^\perp$ belongs to the useless information, so it has the same accuracy as the single-star scheme. In more popular terms, there are only two indicators ΔL and ΔH describing the impact point deviation, which are the reflection of part of the misalignment angle a. When observing a single star, two measurements ξ and η can be obtained, which are also the reflection of part of the misalignment angle a. By selecting the optimal navigation star, ξ and η can include all the information of misalignment angle a contained in ΔL and ΔH. Therefore, the single-star scheme can achieve the same accuracy as the dual-star scheme.

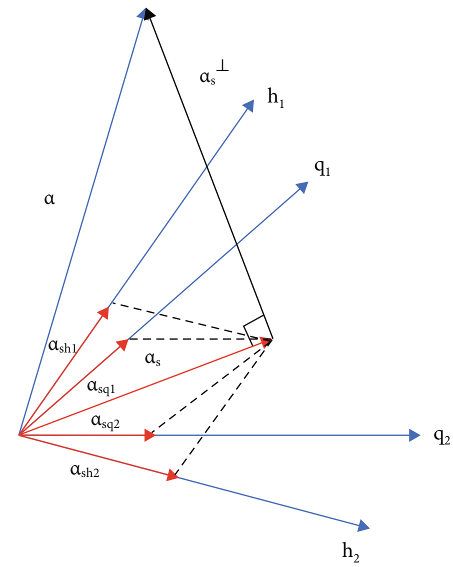

Figure 3: Schematic diagram of determining the optimal navigation star.

3.2. Determining the Optimal Navigation Star. According to the equivalent information compression theory, the optimal navigation star should satisfy

$$h_1 \times h_2 = \frac{q_1 \times q_2}{|q_1 \times q_2|} \text{ or } \quad h_1 \times h_2 = -\frac{q_1 \times q_2}{|q_1 \times q_2|}. \tag{26}$$

For the left side of the above equation, it can be obtained according to the Equation (15).

$$h_1 \times h_2 = [\cos \varphi_0 \cos \psi_0 \quad \sin \varphi_0 \quad \cos \varphi_0 \sin \psi_0]^\mathrm{T}. \tag{27}$$

It is assumed that the star sensor is installed on the *xoy* plane of the platform, and the platform is adjusted to aim at the navigation star by first yaw and then pitch. By substituting$\psi_0 = 0°$ into Equation (27), we can get

$$h_1 \times h_2 = [\cos \varphi_0 \quad \sin \varphi_0 \quad 0]^\mathrm{T}. \tag{28}$$

Define

$$Q_c = [Q_{c1} \quad Q_{c2} \quad Q_{c3}] = q_1 \times q_2, \tag{29}$$

where,

$$\begin{cases} Q_{c1} = (n_{H1}n_{L3} - n_{H3}n_{L1}) \sin \varphi_r + (n_{H3}n_{L2} - n_{H2}n_{L3}) \cos \varphi_r \cos \psi_r + (n_{H1}n_{L2} - n_{H2}n_{L1}) \cos \varphi_r \sin \psi_r, \\ Q_{c2} = (n_{H1}n_{L3} - n_{H3}n_{L1}) \cos \varphi_r - (n_{H3}n_{L2} - n_{H2}n_{L3}) \sin \varphi_r \cos \psi_r - (n_{H1}n_{L2} - n_{H2}n_{L1}) \sin \varphi_r \sin \psi_r, \\ Q_{c3} = -(n_{H1}n_{L2} - n_{H2}n_{L1}) \cos \psi_r + (n_{H3}n_{L2} - n_{H2}n_{L3}) \sin \psi_r. \end{cases} \tag{30}$$

According to Equations (26), (27), and (28), we can get

$$\begin{cases} \psi_r = \tan^{-1}\left(\dfrac{n_{H1}n_{L2} - n_{H2}n_{L1}}{n_{H3}n_{L2} - n_{H2}n_{L3}}\right), \\ \varphi_r = -\tan^{-1}\left(\dfrac{n_{H1}n_{L3} - n_{H3}n_{L1}}{(n_{H2}n_{L3} - n_{H3}n_{L2}) \cos \psi_r + (n_{H2}n_{L1} - n_{H1}n_{L2}) \sin \psi_r}\right) - \varphi_0. \end{cases} \tag{31}$$

The optimal navigation star and the rotation angle satisfy the following relationship:

$$\begin{cases} \sigma_s = -\psi_r, \\ e_s = \varphi_r + \varphi_0. \end{cases} \tag{32}$$

Therefore, the orientation of the optimal navigation star can be expressed as

$$\begin{cases} \sigma_s = -\tan^{-1}\left(\dfrac{n_{H1}n_{L2} - n_{H2}n_{L1}}{n_{H3}n_{L2} - n_{H2}n_{L3}}\right), \\ e_s = -\tan^{-1}\left(\dfrac{n_{H1}n_{L3} - n_{H3}n_{L1}}{(n_{H2}n_{L3} - n_{H3}n_{L2}) \cos \psi_r + (n_{H2}n_{L1} - n_{H1}n_{L2}) \sin \psi_r}\right). \end{cases} \tag{33}$$

According to Equation (26), there is another solution for the orientation of the optimal navigation star.

$$\begin{cases} \sigma'_s = \sigma_s - \pi, \\ e'_s = -e_s. \end{cases} \tag{34}$$

4. Determining the Available Optimal Navigation Star Based on the Star Database

4.1. Angle Analysis of the Deviation from the Optimal Navigation Star. For the single-star platform inertial-stellar composite guidance scheme, only observing the optimal navigation star can achieve the same accuracy as the double star guidance scheme. However, in star database, there are not necessarily stars in the optimal navigation star direction. And only one real star can be selected as the navigation star in the star library according to a certain principle. This star is called the available optimal navigation star. In this section, the angle that the available navigation star deviates from the optimal navigation star is analyzed.

In the i-system, several groups of optimal navigation stars are randomly generated, in which the elevation angles are evenly distributed within $[-90^\circ, \quad 90^\circ]$, and azimuth angles are evenly distributed within $[-180^\circ, \quad 180^\circ]$. Each combination of elevation angles and azimuth angles $[e_{Ni}, \quad \sigma_{Ni}]$ represents a group of possible optimal navigation star, and its direction vector in the i-system is

$$V_{Ni} = \begin{bmatrix} \cos e_{Ni} \cos \sigma_{Ni} & \cos e_{Ni} \sin \sigma_{Ni} & \sin e_{Ni} \end{bmatrix}^{\mathrm{T}}. \tag{35}$$

For any star above 5.5 mag in the star database, its elevation angle and azimuth angle are $[e_{Sj}, \quad \sigma_{Sj}]$; then, the direction vector in the i-system can be expressed as

$$V_{Sj} = \begin{bmatrix} \cos e_{Sj} \cos \sigma_{Sj} & \cos e_{Sj} \sin \sigma_{Sj} & \sin e_{Sj} \end{bmatrix}^{\mathrm{T}}. \tag{36}$$

The angle between the optimal navigation star and the available navigation star can be calculated according to the following equation:

$$\alpha_{ij} = \arccos\left(V_{Ni} \cdot V_{Sj}\right). \tag{37}$$

By traversing j, the minimum angular distance between the optimal navigation star and the available navigation star can be obtained.

100000 samples are sampled, and the results are shown in Figures 4 and 5.

Figures 4 and 5, respectively, show the statistical histogram and probability density histogram of the angles that the available navigation stars deviate from the optimal navigation star. Here, each straight bar represents 0.1°, and the sum of all the sampling times is 100000. In Figure 4, the angular deviations are between 0 and 6° mostly, which mainly concentrated in 1°~3° and relatively few more than 5° or less than 1°. Compared with Figure 4, the shapes of the statistical histogram and probability density histogram are basically the same. Figure 5 also shows the probability density function diagram of the corresponding normal distribution. However, it is obvious that the distribution is not quite consistent with the normal distribution.

Tables 1 and 2 provide the corresponding numerical statistical results. It can be seen from Table 1 that the maximum deviation angle is 7.4221° and the mean deviation angle is 2.0949°. The more detailed statistical analysis results of the available navigation star deviation from the optimal navigation star are illustrated in Table 2. The table counts the single probability and cumulative probability of the deviation angle. It can be observed that $2^\circ > \alpha \geqq 1^\circ$ is the most, accounting for 33.558% and the deviation angle greater than 7° accounts for only 0.014%.

Therefore, if the upper limit of star-sensitive measurement magnitude is 5.5 mag, the available navigation star can be found within the angular distance range within 7° from the optimal navigation star.

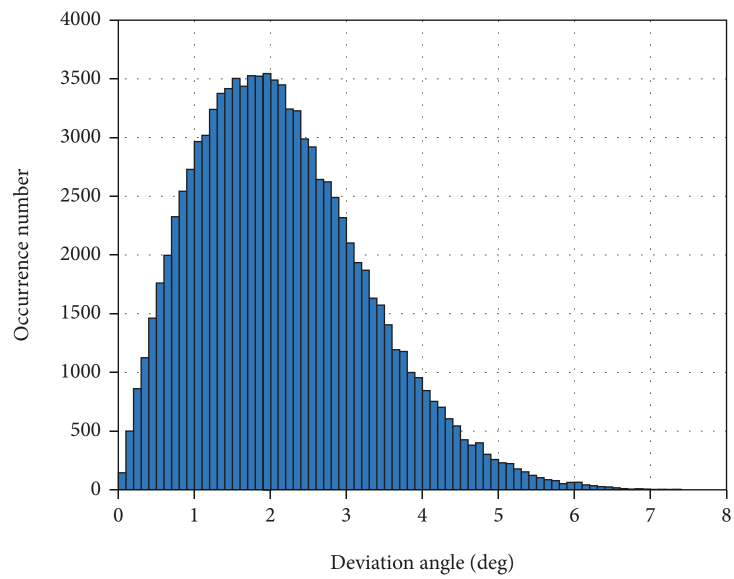

Figure 4: Statistical histogram of the angles that the available navigation stars deviate from the optimal navigation star.

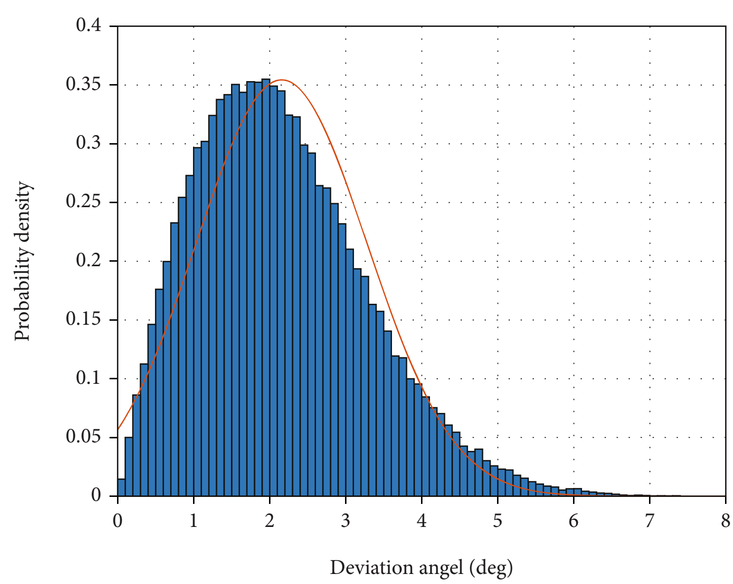

Figure 5: Probability density histogram of the angles that the available navigation stars deviate from the optimal navigation star.

Table 1: The basic analysis results of the available navigation star deviation from the optimal navigation star.

Event	Maximum	Minimum	Mean	Square	3σ range
Value (deg)	7.4221	0.0041	2.0949	1.1139	[-1.2467, 5.4365]

In the above analysis, constraints such as occlusion of the sun, moon, and earth have not been taken into account, and the deviation angle will be much larger after consideration.

4.2. Determining the Available Optimal Navigation Star Based on the Arrow-Borne Navigation Star Database. In practical application, the navigation star must be selected in the arrow-borne navigation star database. According to the above analysis, within the range of 7° from the theoretical optimal navigation star, the probability of finding the navigation star is 100%. Therefore, a method determining the available optimal navigation star based on the local navigation star database is proposed to improve the efficiency of star selection.

4.2.1. Determining the Local Navigation Star Database. Strong light sources should be avoided when determining the local navigation star database (this paper takes avoiding the sun as an example). The right ascension and declination of the sun obtained from the ephemeris table are defined as α_{sun} and δ_{sun}, and the unit sun direction vector in the i

Table 2: statistical analysis results of the available navigation star deviation from the optimal navigation star.

Deviation angle	Number	Probability (%)	Cumulative number	Cumulative probability (%)
$1^\circ > \alpha \geqq 0^\circ$	15449	15.449	15449	15.449
$2^\circ > \alpha \geqq 1^\circ$	33558	33.558	49007	49.007
$3^\circ > \alpha \geqq 2^\circ$	29392	29.392	78399	78.399
$4^\circ > \alpha \geqq 3^\circ$	14842	14.842	93241	93.241
$5^\circ > \alpha \geqq 4^\circ$	5216	5.216	98457	98.457
$6^\circ > \alpha \geqq 5^\circ$	1289	1.289	99746	99.746
$7^\circ > \alpha \geqq 6^\circ$	240	0.240	99986	99.986
$\alpha \geqq 7^\circ$	14	0.014	100000	100.000

Table 3: The value of each error in the simulation.

Error types	Error symbols	Value (3σ)	Units
	ε_{0x}	100	
Initial orientation (alignment) error	ε_{0y}	300	$('')$
	ε_{0z}	100	
Star sensor measurement error	ε_ξ, ε_η	0	$('')$
Star sensor installation error	$\Delta\varphi_0$, $\Delta\psi_0$	0	

-system can be expressed as

$$i_I = \begin{bmatrix} \cos\delta_{\text{sun}} \cos\alpha_{\text{sun}} \\ \cos\delta_{\text{sun}} \sin\alpha_{\text{sun}} \\ \sin\alpha_{\text{sun}} \end{bmatrix}, \quad (38)$$

where i_I is the unit sun direction vector in the i-system.

Then, the unit sun direction vector in the A-system can be further obtained:

$$i_{\text{sun}} = C_I^A \cdot i_I, \quad (39)$$

where i_{sun} is the unit sun direction vector in the A-system and C_I^A is the transformation matrix from the i-system to the A-system.

Therefore, the angular distance θ_s between the theoretical optimal navigation star and the sun can be calculated as

$$\theta_s = \arccos\left(S_I \cdot i_{\text{sun}}\right). \quad (40)$$

If θ_s is less than the sum of the solar avoidance angle α_{sun} and deviation angle $\Delta\alpha$, the deviation angle can be recalculated according to the following equation:

$$\Delta\beta = \frac{-\alpha_{\text{sun}}}{\alpha_{\text{sun}} + \Delta\alpha}\theta_s + \left(\alpha_{\text{sun}} + \Delta\alpha\right), \quad (41)$$

where $\Delta\beta$ is the recalculated deviation angle.

The navigation star orientation in the star database is defined as $[e_0 \quad \sigma_0]$, and its unit vector in the A-system can be expressed as

$$i_0 = \begin{bmatrix} \cos e_0 \cos\sigma_0 \\ \sin e_0 \\ \cos e_0 \sin\sigma_0 \end{bmatrix}. \quad (42)$$

Then, the angular distance θ_I between the navigation star and the theoretical optical navigation star and the angular distance θ_0 between the navigation star and the sun can be calculated, respectively.

$$\begin{cases} \theta_I = \arccos\left(i_0 \cdot S_I\right), \\ \theta_0 = \arccos\left(i_0 \cdot i_{\text{sun}}\right). \end{cases} \quad (43)$$

Therefore, the value of θ_I and the deviation angle can be compared, so as θ_0 and α_{sun}.

$$\begin{cases} \theta_I < \Delta\alpha, & \theta_s \geq \alpha_{\text{sun}} + \Delta\alpha, \\ \theta_I < \Delta\beta, & \theta_s < \alpha_{\text{sun}} + \Delta\alpha, \\ \theta_0 > \alpha_{\text{sun}}. \end{cases} \quad (44)$$

If the above equation is valid, it means that the navigation star is within the deviation angle range of the optimal navigator star and outside the sun avoidance angle range. And the navigation star can be put into the local navigation star database. After calculating all the navigation stars in the star database, the local star database for determining the available optimal navigation star can be obtained.

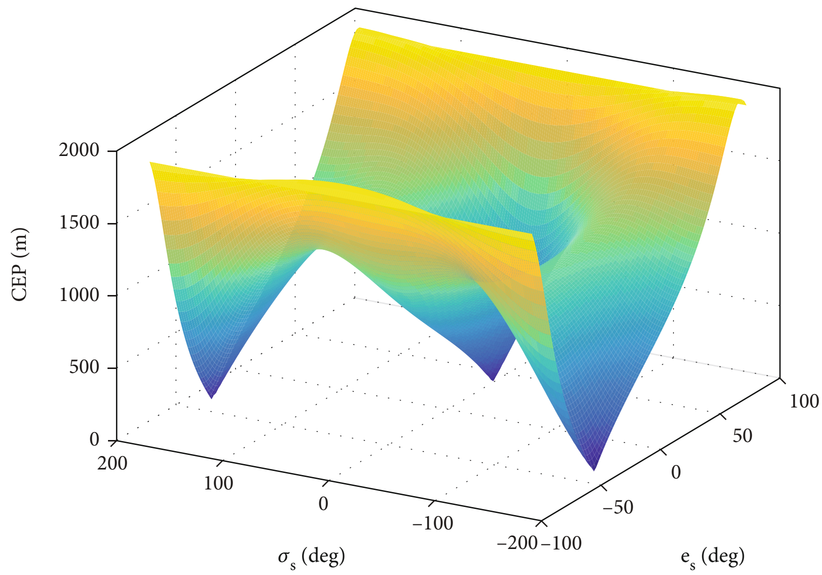

FIGURE 6: Composite guidance CEP variation diagram for 6000 km.

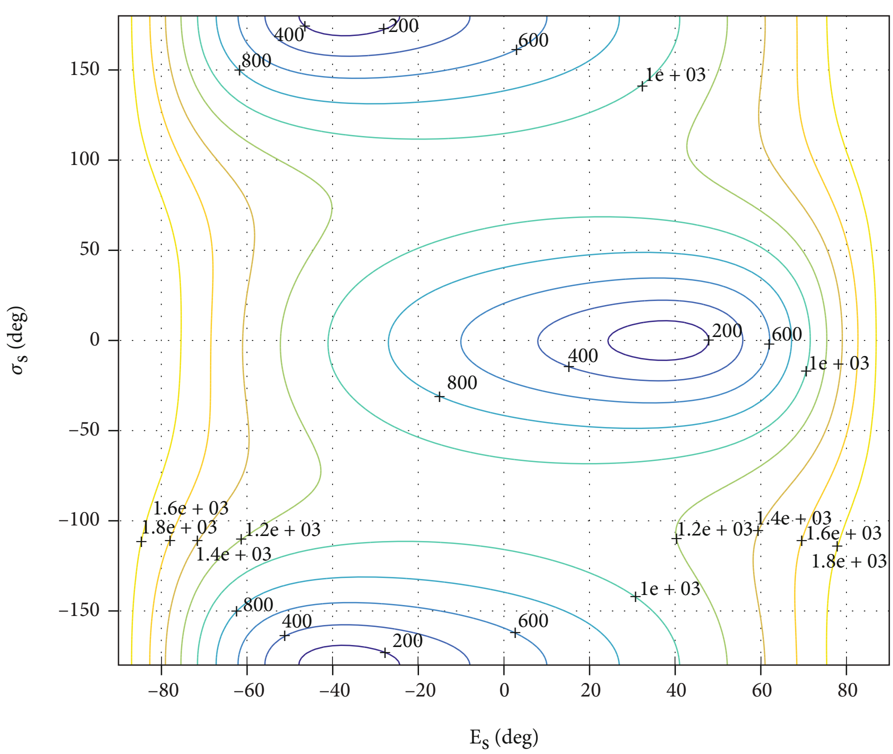

FIGURE 7: Composite guidance CEP contour map for 6000 km.

4.2.2. Determining the Available Optical Navigation Star. Considering that the navigation star with the smallest angular distance from the theoretical optimal navigation star is not necessarily the available optimal navigation star, this paper utilizes the combination of minimum angular distance and minimum accuracy change to determine the available optimal navigation star. Firstly, the angular distance between the stars in the local navigation star database and the optimal navigation star is calculated, and the one with the smallest angular distance is the first available navigation star. Secondly, estimate the accuracy variation of any star in the local navigation star database, and the smallest is the second available navigation star. The calculation method for estimating the accuracy change caused by navigation star deviation is as follows.

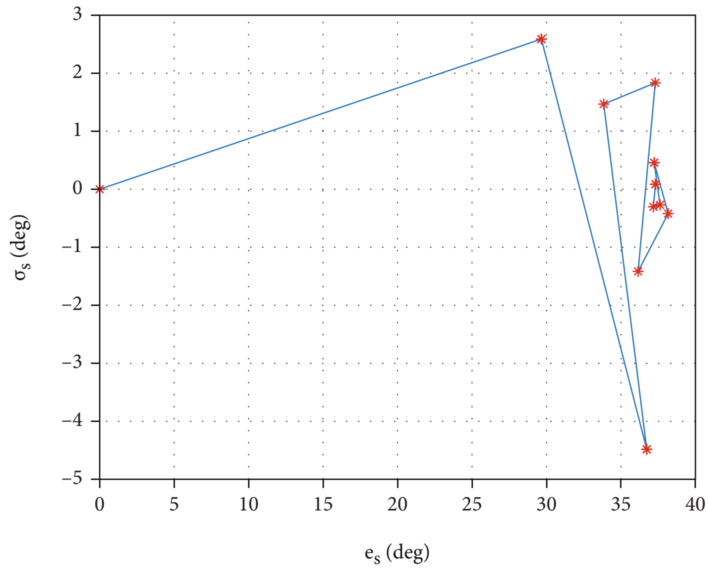

Figure 8: Simplex optimal vertex iterative change diagram with a range of 6000 km.

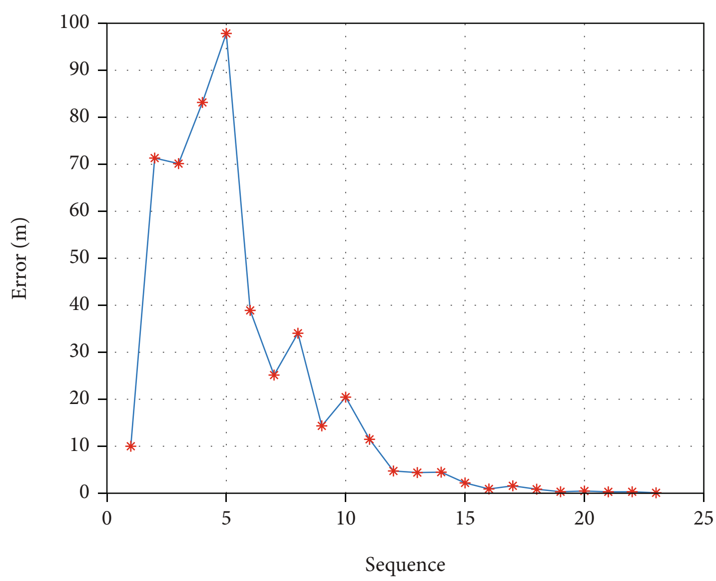

Figure 9: Simplex convergent error variation diagram with a range of 6000 km.

Table 4: Optimal navigation star at different range.

Range	Method	e_s (deg)	σ_s (deg)	CEP_{INS} (m)	CEP_{COM} (m)	t (s)
6000km	Traversing	38	0	2628.89	6.78	2963.05
	Simplex	37.6011	-0.0411	2628.89	0.013	12.09
	Analysis	37.6011	-0.0404	2628.89	0.001	0.001
12000km	Traversing	30	0	3198.36	4.02	2985.53
	Simplex	30.0226	-0.1316	3198.36	0.015	13.22
	Analysis	30.0264	-0.1318	3198.36	0.001	0.003

The gradient can be calculated from the partial derivative of the composite guidance accuracy at the optimal navigation star varying with the navigation star orientation.

$$d_{\nabla} = \frac{\partial \mathrm{CEP}}{\partial e_s} i + \frac{\partial \mathrm{CEP}}{\partial \sigma_s} j, \quad (45)$$

where CEP is the circular error probable and $\partial \mathrm{CEP}/\partial e_s$ and $\partial \mathrm{CEP}/\partial \sigma_s$ are the partial derivative of composite guidance CEP to elevation and azimuth angle at the optimal navigation star. The direction perpendicular to the gradient is the direction with the slowest change in the composite guidance accuracy.

$$d_{\nabla}^{\perp} = -\frac{\partial \mathrm{CEP}}{\partial \sigma_s} i + \frac{\partial \mathrm{CEP}}{\partial e_s} j. \quad (46)$$

Therefore, for any star in the local navigation star database, the accuracy change ΔCEP can be estimated according to

$$\Delta \mathrm{CEP} = \sqrt{\left(\frac{\partial \mathrm{CEP}}{\partial \sigma_s} \Delta e_s\right)^2 + \left(\frac{\partial \mathrm{CEP}}{\partial e_s} \Delta \sigma_s\right)^2}, \quad (47)$$

where Δ CEP is the estimated value of the accuracy change between the navigation star and the optimal navigation star. Δe_s and $\Delta \sigma_s$ are the difference of elevation angle and azimuth angle between the star in the local navigation star database and the optimal navigation star. When the star is smallest, it is selected as the second available navigation star. For the first and the second available navigation star, the one with smaller CEP is the available optimal navigation star.

5. Simulation Results

This section mainly include two parts: (1) determining the theoretical optimal navigation star and (2) determining the available optimal navigation star based on the star database. The simulations are primarily aimed at verifying the effectiveness of the proposed method.

In the simulation, two representative responsive launch vehicle trajectories are adopted. The launch time is 00 : 00 : 00, 1 January 2019 (UTC). The first whole flight time is 1300 s, and the second whole flight time is 2300 s. The initial position is (0°N, 0°E). The star sensor works beyond the atmosphere. And the star sensor installation angle is $[\varphi_0, \psi_0] = [20^\circ, 0^\circ]$. The simulation parameters for the initial alignment error and star sensor error are listed in Table 3. Two trajectories can better verify the effectiveness of the proposed method.

5.1. Determining the Optimal Navigation Star. This section is used to evaluate the effectiveness of the algorithm in Section 3. In the simulation, the optimal navigation star is determined by three methods, which are traversal method, simplex evolutionary method, and analytical method proposed in this paper.

The traversal method searches in the full dimensional space with $-90^\circ \le e_s \le 90^\circ$ and $-180^\circ < \sigma_s \le 180^\circ$, and the step is 1°. Taking the 6000 km trajectory (first trajectory) as an example, when the optimal navigation star is determined by the traversal method, the composite guidance accuracy under different measurement orientations is shown in Figure 6, and the composite guidance CEP contour is shown in Figure 7.

Table 5: Optimal navigation stars with different star sensor installation error.

$\Delta\varphi_0$, $\Delta\psi_0$ $('', 3\sigma)$	Method	e_s (deg)	σ_s (deg)
0	Simplex	37.6011	-0.0411
	Analysis	37.6011	-0.0404
10	Simplex	37.5998	-0.0417
	Analysis	37.6011	-0.0404
20	Simplex	37.5991	-0.0423
	Analysis	37.6011	-0.0404
30	Simplex	37.5979	-0.0440
	Analysis	37.6011	-0.0404

Table 6: Optimal navigation star with different star sensor measurement error.

ε_ξ, ε_η $('', 3\sigma)$	Method	e_s (deg)	σ_s (deg)
0	Simplex	37.6011	-0.0411
	Analysis	37.6011	-0.0404
10	Simplex	37.6011	-0.0404
	Analysis	37.6011	-0.0404
20	Simplex	37.6012	-0.0403
	Analysis	37.6011	-0.0404
30	Simplex	37.6012	-0.0404
	Analysis	37.6011	-0.0404

Figure 6 shows the composite guidance CEP variation diagram for 6000 km. It can be observed that there are two minimum points in the composite guidance accuracy variation diagram corresponding to the single-star tuning platform; that is, there are two optimal navigation stars. And the two optimal navigation stars azimuth is approximately on the same line as the emission point, that is, $e'_s = -e_s$ and $\sigma'_s = \sigma_s - \pi$. This is consistent with the analysis conclusion of Equation (33). Besides, the composite guidance accuracy is approximately symmetric with respect to the line according to Figure 7.

In the simplex evolutionary method, the initial vertex is $X_0 = [e_{s0} \quad \sigma_{s0}]^{\mathrm{T}} = [20^\circ \quad 0^\circ]^{\mathrm{T}}$. Take the distance between vertices $\Delta d = 10^\circ$ to construct the initial simplex, and the iteration termination condition is taken as $\varepsilon = 0.1$m. The change of the simplex optimal vertex in the iteration process is shown in Figure 8, and the convergence error is shown in Figure 9.

It can be seen from the above figures that when utilizing the simplex evolutionary method to determine the optimal navigation star, the simplex converges quickly in the solution process, and the algorithm has a large search range.

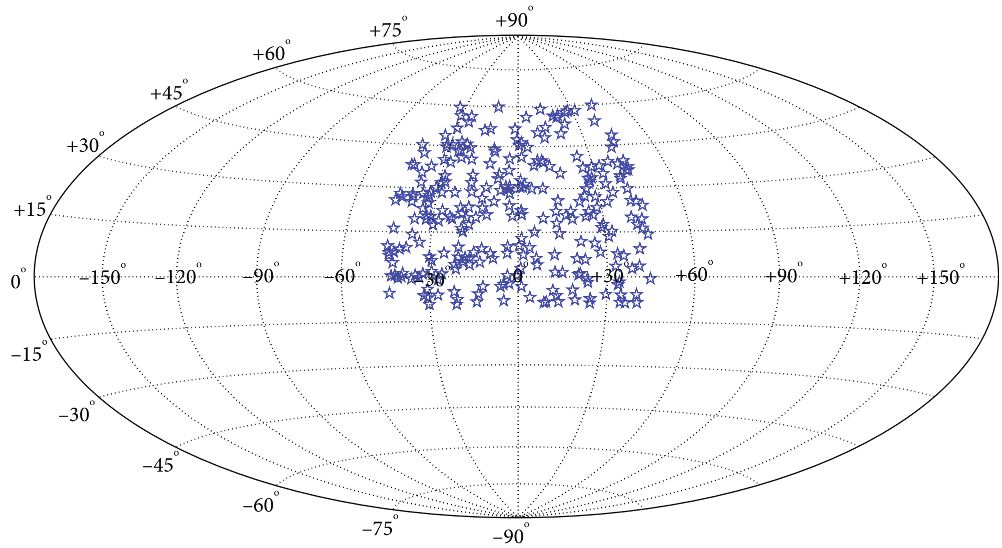

Figure 10: Arrow-borne navigation star database.

Table 7: Local navigation star database.

Number	e_s (deg)	σ_s (deg)	CEP_{INS} (m)	CEP_{COM} (m)
1	35.0459	-7.3824	2628.89	139.409
2	36.4093	-3.5698	2628.89	67.152
3	40.6013	-3.4893	2628.89	83.301
4	32.8418	0.9406	2628.89	79.633
5	41.2134	1.4235	2628.89	69.357
6	31.5162	2.5029	2628.89	108.593
7	38.1545	6.3915	2628.89	117.695
8	39.9243	7.9122	2628.89	150.393

At the same time, it can achieve high accuracy by controlling the convergence domain.

Table 4 represents the required time and the optimal navigation stars determined by the three methods. In the table, CEP_{INS} is the pure inertial guidance accuracy, and CEP_{COM} is the composite guidance accuracy.

The simulation results show that under the condition of only considering the initial alignment error, the results obtained by analytical method are consistent with those obtained by traversal method and simplex evolutionary method, which verify the effectiveness of the proposed method. At the same time, the azimuth angle of the navigation star is about 0°, which indicates that the optimal navigation star is near the shooting plane when the star sensor is installed on the *xoy* plane of the platform.

According to the results of the optimal navigation stars and the corresponding composite guidance accuracy, the accuracy of the traversal method is limited because the traversal method is searched with a fixed step, while the analytic method and simplex evolutionary method have no such limitation. Thus, the optimal navigation star azimuth can achieve high accuracy. When comparing the calculation time of the three methods, the results are calculated on PC. By contrast, the traversal calendar takes about 50 minutes, while the analytic method can be completed in a very short time. And the composite guidance accuracy corresponding to the optimal navigation star obtained by the analytical method is 99.99% (from 6.78 m to 0.001 m) and 92.31% (from 0.013 m to 0.001 m) higher than that obtained by the traversal method and the simplex evolutionary method. Moreover, the time-consuming of the traversal method is related to the traversal step size. The smaller the step size, the more time-consuming, but the more accurate the optimal star azimuth is determined. Therefore, under the condition of significant initial error, the method proposed in this paper can be used to help determine the optimal navigation star quickly. Since only the initial orientation error is considered in the simulation, the stellar guidance can correct all the effects of the error, and the corrected accuracy is close to 0 m. Of course, it is impossible to achieve when all error factors are considered.

Taking the responsive launch vehicle with a range of 6000 km as an example, the influence of the star sensor installation error and measurement error on the optimal navigation star is analyzed. In the simulation, simplex evolutionary method and analytic method are utilized to determine the optimal navigation star. Table 5 represents the optimal navigation stars when considering the star sensor installation error, and Table 6 represents the optimal navigation stars when considering the star sensor measurement error.

The star sensor installation error has a certain impact on the optimal navigation star, but the impact is small. The range of changes in elevation angle and azimuth angle is both within 0.01°. Comparing Tables 5 and 6, it can be seen that the star sensor measurement error has less impact on the optimal navigation star. Therefore, the method proposed in this paper can determine the optimal navigation star effectively.

Table 8: The available optimal navigation stars for the 6000 km launch vehicle.

Date		2019/1/1	2019/3/10	2019/8/20
Theoretical optimal navigation star	e_s (deg)	37.6011	37.6011	37.6011
	σ_s (deg)	-0.0404	-0.0404	-0.0404
	CEP_{INS} (m)	2628.89	2628.89	2628.89
	CEP_{COM} (m)	0.001	0.001	0.001
Available optimal navigation star (traversal method)	e'_s (deg)	36.4093	36.5827	37.0740
	σ'_s (deg)	-3.5698	1.0344	-2.9698
	CEP_{INS} (m)	2628.89	2628.89	2628.89
	CEP_{COM} (m)	67.152	26.320	54.120
Available optimal navigation star (proposed method)	e'_s (deg)	36.4093	36.5827	37.0740
	σ'_s (deg)	-3.5698	1.0344	-2.9698
	CEP_{INS} (m)	2628.89	2628.89	2628.89
	CEP_{COM} (m)	67.152	26.320	54.120

Table 9: The available optimal navigation stars for the 12000 km launch vehicle.

Date		2019/1/1	2019/3/10	2019/8/20
Theoretical optimal navigation star	e_s (deg)	30.0264	30.0264	30.0264
	σ_s (deg)	-0.1318	-0.1318	-0.1318
	CEP_{INS} (m)	3198.36	3198.36	3198.36
	CEP_{COM} (m)	0.001	0.001	0.001
Available optimal navigation star (traversal method)	e'_s (deg)	30.5718	32.2593	25.3675
	σ'_s (deg)	0.7825	0.3548	-0.4691
	CEP_{INS} (m)	3198.36	3198.36	3198.36
	CEP_{COM} (m)	26.332	33.224	64.516
Available optimal navigation star (proposed method)	e'_s (deg)	30.5718	32.2593	25.3675
	σ'_s (deg)	0.7825	0.3548	-0.4691
	CEP_{INS} (m)	3198.36	3198.36	3198.36
	CEP_{COM} (m)	26.332	33.224	64.516

5.2. Determining the Optimal Available Navigation Star. Stars are basically evenly distributed in the celestial coordinate system, and the earth shielding range of in the star sensor view field is basically fixed. Due to the physical realization of the inertial platform frame angle, there will be some restrictions on the azimuth and elevation angles. It is assumed that the azimuth angle has a limit of ±45°, and the elevation angle has a limit of ±60°. At the same time, it is assumed that the sun's avoidance angle is 20°, the moon's avoidance angle is 10°, the horizon's additional avoidance angle is 5°, and the large planet's avoidance angle is 2°. The arrow-borne navigation star database is shown in Figure 10, and the generated local navigation star database based on the Section 4.2.1 is shown in Table 7.

Figure 10 shows the generated arrow-borne navigation star database when the launch time is January 1, 2019. Due to the influence of constraints, the final number of available navigation stars is 292. Compared with Figure 10, it can be seen that there are only 8 alternative navigation stars in the local navigation star database, indicating that most stars in the array-borne navigation star database can be excluded based on the maximum deviation angle from the theoretical optimal navigation star, thus shortening the time to determine the available optimal navigation star. Tables 8 and 9 represent the available optimal navigation stars for the 6000 km and 12000 km launch vehicle.

Table 8 and 9 show the comparison results of the proposed method and the traversal method to determine the available optimal navigation star. The traversal method in the table refers to traversing all stars in the local navigation star database, and the results obtained can be considered as accurate. The proposed method refers to the available optimal navigation star determined according to Section 4.2.2. The above results are the navigation stars selected from the real local navigation star database after considering various star selection constraints. It can be observed from the tables that the navigation star determined by the proposed method is the same as the traversal method, which proves that this method in this paper is effective. At the same, the angular distance between the theoretical optimal navigation star and the available optimal navigation star is within 5°, and the variation of composite guidance accuracy is less than 70 m, indicating that the available optimal navigation star still has a good correction effect.

6. Conclusion

The demand for the application of single-star inertial-stellar guidance system in responsive launch vehicles is to determine the optimal navigation star quickly. However, the current optimal navigation star selection schemes are to determine the star by numerical method, which increase the preparation time before launch. This paper proposes a fast algorithm to determine the star. The key of this algorithm is to deduce the optimal navigation star based on the equivalent information compression theory under the condition of significant initial error. It is obvious that the analytical solution is less time-consuming than the numerical solution. And the analytical solution can achieve the same accuracy as the numerical solution, or even higher.

On the basis of determining the optimal navigation star, the available optimal navigation star should be further determined in combination with the arrow-borne navigation star database. There are certain deviations between the optimal navigation star and the navigation stars in the database. Therefore, the deviation angles between them without considering constraints are analyzed firstly. Based on the deviation angle, the navigation stars are selected to the local navigation database. Then, the available optimal navigation star can be determined according to certain criteria. The algorithm proposed in this paper can quickly determine the optimal navigation star and the available optimal navigation star.

Data Availability

The data used to verify the effectiveness of this method are included within the paper. The data is generated by utilizing the software which is described in Section 5. The data used to support the findings of this manuscript, "A fast algorithm for determining the optimal navigation star for responsive launch vehicles," written by Yi Zhao, Hongbo Zhang, Pengfei Li, and Guojian Tang, is generated by software. The detailed simulation conditions are presented in this paper.

Conflicts of Interest

The authors declare that there is no conflict of interest regarding the publication of this paper.

References

[1] H. B. Zhang, W. Zheng, and G. J. Tang, "Stellar/inertial integrated guidance for responsive launch vehicles," *Aerospace Science and Technology*, vol. 18, no. 1, pp. 35–41, 2012.

[2] S. F. Rounds and G. Marmar, "Stellar-inertial guidance capabilities for advanced ICBM," in *Guidance and Control Conference*, pp. 849–885, Gatlinburg, TN, 1983.

[3] J. Z. Lu, M. Q. Hu, Y. Q. Yang, and M. Dai, "On-orbit calibration method for redundant IMU based on satellite navigation & star sensor information fusion," *IEEE Sensors Journal*, vol. 1, no. 1, pp. 99–114, 2020.

[4] J. A. Christian, "StarNAV: autonomous optical navigation of a spacecraft by the relativistic perturbation of starlight," *Sensors*, vol. 19, no. 19, pp. 4064–4126, 2019.

[5] X. L. Ning, X. H. Sun, and W. Chao, "Integration of star pixel coordinates and their time differential measurement in satellite stellar refraction navigation," *Acta Astronautica*, vol. 159, no. 1, pp. 286–293, 2019.

[6] G. Wahba, "A least squares estimate of satellite attitude," *SIAM Review*, vol. 7, no. 3, pp. 409–415, 1965.

[7] I. Y. Bar-Itzhack and R. R. Harman, "Optimized TRIAD algorithm for attitude determination," *Journal of Guidance Control and Dynamics*, vol. 20, no. 1, pp. 208–211, 1997.

[8] J. L. Farrell, J. C. Stuelpnagel, R. H. Wessner, J. R. Velman, and J. E. Brook, "A least squares estimate of satellite attitude (Grace Wahba)," *SIAM Review*, vol. 8, no. 3, pp. 384–386, 1966.

[9] M. D. Shuster, "Three-axis attitude determination from vector observations," *Journal of Guidance Control and Dynamics*, vol. 4, no. 1, pp. 70–77, 1981.

[10] F. L. Markly, "Attitude determination using vector observations and the singular value decomposition," *Journal of the Astronautical Sciences*, vol. 36, no. 3, pp. 245–258, 1988.

[11] F. L. Markly, "Attitude determination using vector observations: a fast optimal matrix algorithm," *Journal of the Astronautical Sciences*, vol. 42, no. 2, pp. 261–280, 1993.

[12] D. Mortari, "Euler-q algorithm for attitude determination from vector observations," *Journal of Guidance Control and Dynamics*, vol. 21, no. 2, pp. 328–334, 1998.

[13] J. Wu, Z. B. Zhou, H. Fourati, R. Li, and M. Liu, "Generalized linear quaternion complementary filter for attitude estimation from multisensor observations: an optimization approach," *IEEE Transactions on Automation Science and Engineering*, vol. 16, no. 3, pp. 1330–1343, 2019.

[14] J. Wu, Z. B. Zhou, R. Li, Y. Cheng, and H. Fourati, "Fast linear quaternion attitude estimator using vector observations," *IEEE Transactions on Automation Science and Engineering*, vol. 15, no. 1, pp. 307–319, 2018.

[15] J. Wu, Z. B. Zhou, M. Song, H. Fourati, and M. Liu, "Convexity analysis of optimization framework of attitude determination from vector observations," in *2019 6th International Conference on Control, Decision and Information Technologies (CoDIT)*, pp. 440–445, Paris, France, 2019.

[16] H. Yang and L. Carlone, "A quaternion-based certifiably optimal solution to the Wahba problem with outliers," in *IEEE 2019 IEEE/CVF International Conference on Computer Vision (ICCV)*, pp. 1665–1674, Seoul, Korea (South), 2019.

[17] H. Ghadiri, H. Esmaelzadeh, and R. Zardashti, "Robust optimal attitude determination using interval analysis," *Advances in Space Research*, vol. 69, no. 6, pp. 2611–2617, 2022.

[18] J. Wang and J. Chun, "Attitude determination using a single star sensor and a star density table," *Journal of Guidance Control and Dynamics*, vol. 29, no. 6, pp. 1329–1338, 2006.

[19] D. Wang, H. Lv, X. An, and J. Wu, "A high-accuracy constrained SINS/CNS tight integrated navigation for high- orbit automated transfer vehicles," *Acta Astronautica*, vol. 151, no. 10, pp. 614–625, 2018.

[20] J. Wu, Z. B. Zhou, R. Li, L. Yang, and H. Fourati, "Attitude determination using a single sensor observation: analytic quaternion solutions and property discussion," *IET Science, Measurement & Technology*, vol. 11, no. 6, pp. 731–739, 2017.

[21] C. G. Xiao, "Strapdown celestial guidance scheme and precision analysis," *Missiles Space Vehicles*, vol. 4, pp. 1–8, 1997.

[22] Z. S. Jin and G. X. Shen, "Study on stellar-inertial integrated guidance system for mobile ballistic missile," *ACTA Aeronautica ET Astronautica Sinica*, vol. 26, no. 2, pp. 168–172, 2005.

[23] H. Zhang, W. Zheng, J. Wu, and G. Tang, "Investigation on single-star stellar-inertial guidance principle using equivalent information compression theory," *Science in China Series E: Technological Sciences*, vol. 52, no. 10, pp. 2924–2929, 2009.

[24] B. Ye, H. B. Zhang, and J. Wu, "Study on quick ascertaining method of optimal single star in celestial-inertial integrated guidance," *Journal of Astronautics*, vol. 30, no. 4, pp. 1371–1375, 2009.

[25] J. Zhang, Z. Wang, X. H. Chang, and B. Hong, "Research on inertial/celestial integrated guidance system of single star," *Astronautical Systems Engineering Technology*, vol. 1, no. 2, pp. 7–11, 2017.